Effects of isomer coexistence and solvent-induced core switching in the photodissociation of bare and solvated $(CS_2)_2^-$ anions

Terefe Habteyes,[a] Luis Velarde,[b] and Andrei Sanov[c]
Department of Chemistry, University of Arizona, Tucson, Arizona 85721-0041, USA

(Received 31 December 2008; accepted 13 February 2009; published online 23 March 2009)

The photodissociation of the $(CS_2)_2^-$ dimer anion, known to exist in the form of several electronic and structural isomers, has been investigated at 532, 355, and 266 nm. The observed anionic fragments are CS_2^- and $C_2S_2^-$ at 532 nm, and $C_2S_2^-$, CS_2^-, CS_3^-, S_2^-, and S^- at 355 and 266 nm. In addition to the photon energy, the fractional yields of the photofragments depend on the ion source conditions and solvation of the dimer anion. Specifically, the $(C_2S_2^- + S_2^-)/CS_2^-$ product ratio is significantly higher when $(CS_2)_2^-$ is formed in the presence of water in the precursor gas mixture, even though the parent anion itself does not include H_2O. On the other hand, an abrupt decrease in the above product ratio is observed upon the addition of solvent molecules (CS_2 or H_2O) to the $(CS_2)_2^-$ anion. Since the variation of this product ratio exhibits positive correlation with the relative intensity of the photoelectron band assigned to the C_{2v} $(^2B_1)$ covalent structure of $C_2S_4^-$ by Habteyes *et al.* [J. Phys. Chem. A **112**, 10134 (2008)], this structure is suggested as the primary origin of the $C_2S_2^-$ and S_2^- photoproducts. The switching of the fragmentation yield from $C_2S_2^-$ and S_2^- to other products upon solvation is ascribed to the diminished presence of the C_{2v} $(^2B_1)$ dimer-anion structure relative to the CS_2^- based clusters. This population shift is attributed to the more effective solvation of the latter. The CS_2^- based clusters are suggested as the origin of the S^- photoproduct, while CS_3^- is formed through the secondary $S^- + CS_2$ intracluster association reaction. © *2009 American Institute of Physics*. [DOI: 10.1063/1.3094318]

I. INTRODUCTION

Carbon disulfide is used as a solvent and a building block in the synthesis of many organic compounds. The reactivity of CS_2 can be contrasted with that of isovalent CO_2 by referring to the thermochemical data on ion-molecule association and clustering reactions.[1] Carbon dioxide forms weakly bound complexes with positive ions due to the poor Lewis basicity of oxygen atoms, but it forms covalent bonds with negative ions (such as O^-) through nucleophilic attack on the carbon atom.[2,3] The CS_2 molecule, on the other hand, exhibits amphoteric character, forming covalent bonds with both positive and negative ions through its sulfur and carbon atoms, respectively.[4] In the gas-phase clustering reactions of CS_2 in a pulsed electron-beam high-pressure mass spectrometer, S_2^-, $S_2^- \cdot CS_2$, and CS_3^- ions were observed as minor products, in addition to the $(CS_2)_n^-$ clusters.[4] In the drift-tube study of the $^{34}S^- + CS_2$ reaction, the isotope-exchange ($S^- + {}^{34}SCS$) and sulfur abstraction ($^{34}SS^- + CS$) products were observed.[5] Although CS_3^- was not detected directly, the formation of the long-lived CS_3^{-*} complex was suggested in the isotope-exchange process. However, in the S_2^- channel, which was observed at collision energies above 0.3 eV, the $^{32}S\ ^{32}S^-$ product was not observed, ruling out the formation of an intermediate CS_2^{-*} collision complex.[5]

Maeyama *et al.*[6] studied the photodissociation of $(CS_2)_n^-$, $n=1-4$, in the ~1.0–2.8 eV photon energy range. Two dissociation channels, $CS_2^- + CS_2$ and $C_2S_2^- + S_2$, were observed for $n \geq 2$. Although the channel branching ratios could not be quantified, it was suggested that the same cluster core was involved for all n in the $n=2-4$ range, as the total photodepletion cross section peaked between 1.6 and 1.8 eV for all the clusters studied. These results were interpreted[6] considering the $C_2S_4^-$ structure of C_{2v} symmetry (corresponding to the $^2B_1$ electronic state), in which the two CS_2 moieties are bound by the covalent C–C and S–S bonds. This dimer-anion structure (shown in Fig. 1) had been predicted earlier[4] based on theoretical calculations. The photoelectron spectra measured by Tsukuda *et al.*[7] confirmed the existence of the covalent dimer-anion. The bands corresponding to the CS_2^- and $C_2S_4^-$ based clusters were observed for $(CS_2)_n^-$ with n up to 6. In the intracluster reactions of $(CS_2)_n^-$ induced by surface impact at a collision energy of 50 eV, Kondow and co-workers[8] observed the S^-, C_2S^-, S_2^-, CS_2^-, and $C_2S_2^-$ fragments for $n=2$, and S^-, S_2^-, and CS_2^- for $n=3$.

In addition to the above C_{2v} $(^2B_1)$ structure,[4,6,9] other isomers have been proposed for $(CS_2)_2^-$, which include several distinct covalently bound structures.[7,10–13] Recently, we reported a photoelectron imaging study of $(CS_2)_2^-$ under varying ion-source and solvation conditions.[14] With the aid of theoretical calculations,[15] the bands in the photoelectron images and spectra were assigned to the $CS_2^- \cdot CS_2$ ion-molecule complex and two covalent structures, C_{2v} $(^2B_1)$ and D_{2h} $(^2B_{3g})$, shown in Fig. 1. The C_{2v} $(^2B_1)$ isomer was con-

[a]Present address: Department of Chemistry, University of California, Berkeley, CA 94720-1460, USA.
[b]Present address: Department of Chemistry, University of California, Santa Barbara, CA 93106-9510, USA.
[c]Author to whom correspondence should be addressed. Electronic mail: sanov@u.arizona.edu.

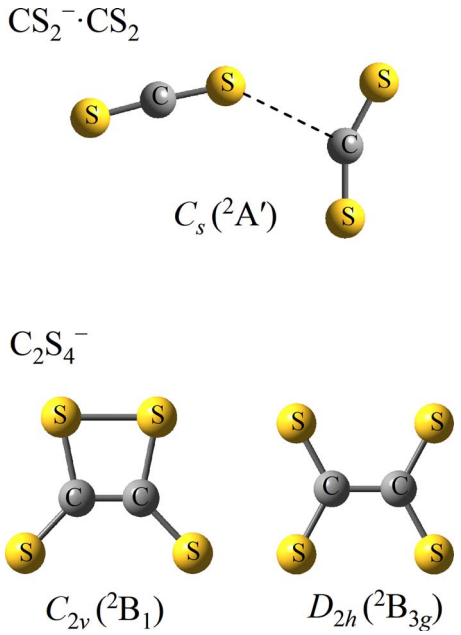

FIG. 1. (Color online) Stable structures of $(CS_2)_2^-$ taken from Ref. 14. See the text for details.

firmed as the global-minimum structure, but the actual isomer distribution was found to depend sensitively on the ion source conditions, particularly the presence of small amounts of water in the precursor gas mixture.

In this report, building on the previous work,[14] we explore the manifestations of the different electronic-structural properties of the coexisting $(CS_2)_2^-$ isomers in the photochemistry of this complex system. The photodissociation of $(CS_2)_2^-$, as well as the $(CS_2)_n^-$, $n \leq 4$, and $(CS_2)_2^-\cdot(H_2O)_m$, $m \leq 2$ cluster anions is investigated using tandem time-of-flight parent and fragment mass spectroscopy. The channel branching ratios are analyzed under varying ion-source conditions (affecting the parent isomer distribution) and cluster solvation. The results shed light not only on the photoinduced reactivity, but also on the structure of the parent anions, complementing the photoelectron imaging study.[14]

II. EXPERIMENTAL

The experiments are carried out using the negative-ion tandem time-of-flight mass spectrometer described elsewhere.[16] Neutral clusters of CS_2 are formed by passing Ar carrier gas at 40 psi over a liquid sample of carbon disulfide. The resulting mixture is expanded through a 0.8 mm orifice pulsed nozzle operating at a 50 Hz repetition rate into a vacuum chamber with a base pressure of 2×10^{-7} Torr. Several millimeters downstream from the nozzle orifice, the supersonic expansion is crossed with a continuous beam of 1 keV electrons. Negative ions are formed by secondary electron attachment to neutral clusters.[17]

Two types of ion-source conditions are used in the reported experiments. In the subsequent discussion, "dry source" refers to the regime where moisture in the precursor gas delivery line has been removed as much as possible by means of baking and pumping. Alternatively, in order to generate hydrated cluster anions, a droplet of water is added to the precursor delivery line, corresponding to the so-called "wet source conditions." Under the dry conditions, the $(CS_2)_n^-$ cluster progression is most abundant in the parent-ion mass spectra. With the "wet" source, the $(CS_2)_n^-(H_2O)_m$ cluster anions are most prominent (see Fig. 2 in Ref. 14).

The negative ions are pulse extracted from the source chamber into the 2.3 m long flight tube of a Wiley–McLaren time-of-flight mass spectrometer. The ions are accelerated to a kinetic energy of about 3 keV and brought to a temporal and spatial focus in the detection region of the instrument with a base pressure of 5×10^{-9} Torr, where they are detected with an in-line microchannel plate (MCP) detector mounted at the end of the flight tube.

A pulsed laser beam is timed to overlap with the mass-selected cluster anions of interest and the resulting photofragments are mass analyzed using a reflectron time-of-flight mass spectrometer and a second off-axis MCP detector.[16] The experiments are performed with the 532, 355, and 266 nm harmonics of a neodymium-doped aluminum garnet laser (Spectra Physics Laboratory 130, 50 Hz pulse repetition rate), with approximate pulse energies of 30, 15, and 5 mJ, respectively. The photofragment mass spectra are recorded by accumulating the pre-amplified ion signals from the off-axis MCP detector over 512 experimental cycles using a digital oscilloscope.

III. RESULTS

In Sec. III A, we describe the photofragmentation pathways of hydrated CS_2^- ions. These results set the stage for the discussion of the contrasting fragmentation patterns of cluster anions containing the CS_2^- and $C_2S_4^-$ ionic cores (Sec. III B). In Sec. III C, the effect of the formation conditions on the fragmentation pathways of (nominally) the same cluster anions is considered.

A. Photodissociation of bare and hydrated CS_2^-

The photofragment-ion mass spectra for the $CS_2^-(H_2O)_m$ parent anions collected at 355 and 266 nm are presented in Figs. 2(a) and 2(b), respectively. The spectra are normalized to the same maximum intensity not representative of the absolute dissociation cross sections. At 355 nm, the S^- based products appear for $m=0-5$. As m increases, the CS_2^- fragment is first seen for $m=2$ and its hydrates become the only observed product type for $m=6-8$. At 266 nm, no anionic photofragments are observed for $m=0$ and 1, indicating that a minimum of two water molecules is required to enable the photodissociation, as opposed to the photodetachment of CS_2^- at this wavelength. The 266 nm fragments observed for $m \geq 2$ are similar to the 355 nm results, with a slight variation in the relative peak intensities.

B. Photofragmentation of $(CS_2)_n^-$ and $(CS_2)_2^-(H_2O)_m$ cluster anions

The photofragment mass spectra for the $(CS_2)_n^-$, $n=2-4$, and $(CS_2)_2^-(H_2O)_m$, $m=0-2$ parent anions obtained at 532, 355, and 266 nm are presented in Figs. 3(a) and 3(b), respectively. While the fragment distributions depend, as expected, on photon energy and the number of solvating CS_2 or

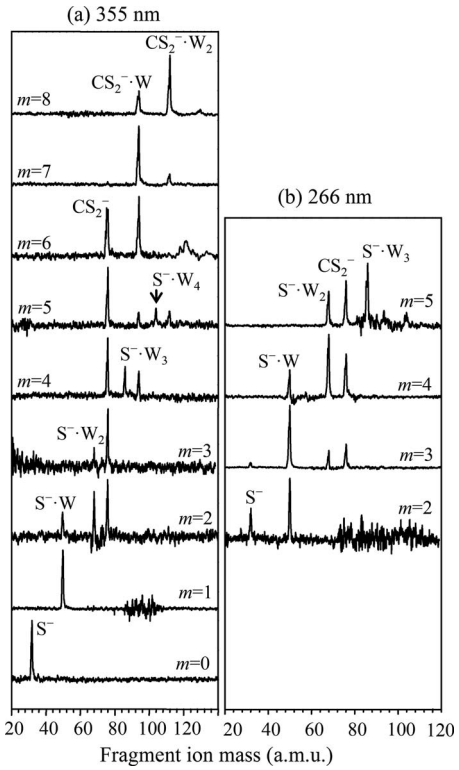

FIG. 2. The 355 and 266 nm photofragment mass spectra for the $CS_2^-(H_2O)_m$ parent ions. $W \equiv H_2O$.

H_2O molecules, they also exhibit a less intuitive, yet significant, dependence on the ion source conditions, specifically the presence of water in the precursor gas mixture. The spectra in Fig. 3(a) were obtained under the dry source conditions, while those in Fig. 3(b) correspond to the wet source conditions. The moisture effect on the fragmentation of (nominally) the same parent anion, $(CS_2)_2^-$, can be seen by comparing the $n=2$ spectra in Fig. 3(a) to the corresponding $m=0$ spectra in Fig. 3(b). Of the several photofragment types, we particularly emphasize the relative yields of CS_2^-, on the one hand, and $C_2S_2^-$ and S_2^-, on the other. The $(C_2S_2^- + S_2^-)/CS_2^-$ product ratios determined for the different wavelengths and parent ions are summarized in histogram form in Fig. 4.

As also seen in Fig. 3, the simplest fragmentation patterns are observed at 532 nm. At this wavelength, $(CS_2)_2^-$ dissociation yields the CS_2^- and $C_2S_2^-$ fragment ions with comparable intensities regardless of the source conditions. However, upon solvation with additional CS_2 or H_2O molecules, the $C_2S_2^-$ channel is effectively turned off, as reflected in the 532 nm spectra in Fig. 3(a) for $n=3-4$ and Fig. 3(b) for $m=1-2$.

At 355 nm, the S_2^- and CS_3^- anionic fragments are also observed for $(CS_2)_n^-$, in addition to the CS_2^- and $C_2S_2^-$ products. The $C_2S_2^-$ ion is the most intense 355 nm photofragment for the $(CS_2)_2^-$ parent anion. However, with the addition of just one more CS_2 solvent molecule, the $C_2S_2^-$ and S_2^- product channels decrease significantly. Similar to the 532 nm result, in larger clusters the CS_2^- fragment takes a central stage, as seen in Fig. 3(a) for $n=3-4$.

At 266 nm, the $C_2S_2^-$ channel remains dominant for

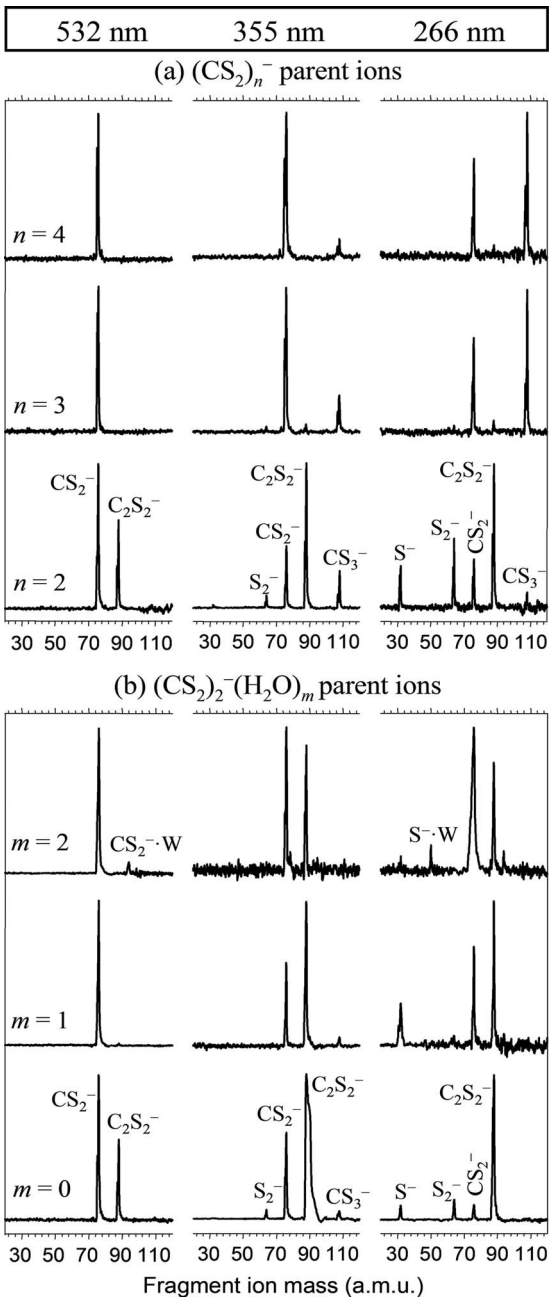

FIG. 3. The photofragment mass spectra for (a) the $(CS_2)_n^-$, $n=2-4$, parent ions and (b) the $(CS_2)_2^-(H_2O)_m$, $m=0-2$, parent ions. The parent anions in (a) and (b) are formed under dry and wet source conditions, respectively.

fragmentation of $(CS_2)_2^-$ under both the dry and wet source conditions, while the CS_2^- yield diminishes further compared to the 355 and 532 nm results. This trend is accompanied by a relative increase in S_2^- and the appearance of the S^- product. Again, the addition of the CS_2 solvent turns off, nearly completely, the S_2^- and $C_2S_2^-$ product channels, along with S^-, while enhancing the relative intensities of CS_2^- and CS_3^-.

C. The effect of water in the ion source

As seen in Figs. 3(a) and 3(b), CS_2^- is the only 532 nm anionic product for both the $(CS_2)_n^-$, $n=3-4$, and $(CS_2)_2^-(H_2O)_m$, $m=1-2$ cluster anions, with the exception

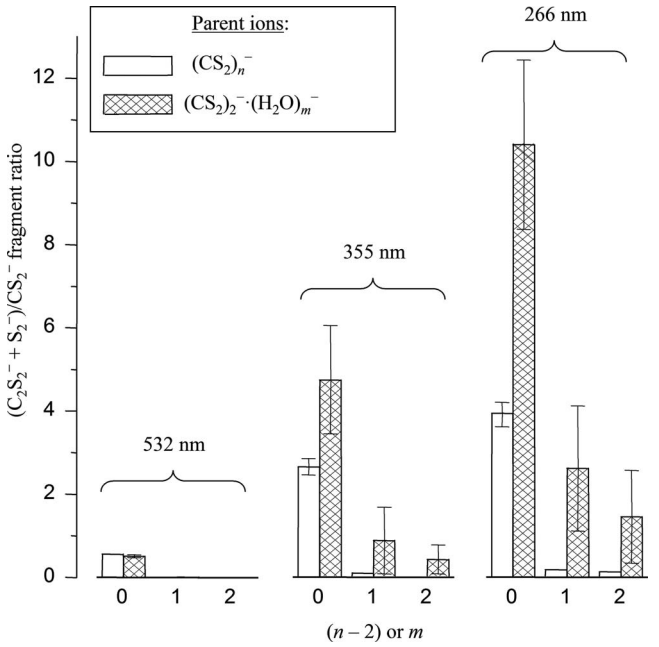

FIG. 4. The $(C_2S_2^- + S_2^-)/CS_2^-$ product ratio for the $(CS_2)_n^-$, $n=2-4$, and $(CS_2)_2^-(H_2O)_m$, $m=0-2$, parent ions, formed under the dry and wet source conditions, respectively.

of a minor $CS_2^-\cdot H_2O$ signal observed for $(CS_2)_2^-(H_2O)_2$. At 355 and 266 nm, however, the fragmentation patterns of the hydrated clusters are drastically different from those of $(CS_2)_n^-$. Even the unhydrated $(CS_2)_2^-$ parent anion exhibits different channel branching ratios depending on the ion source conditions. The $C_2S_2^-$ product fraction is larger for the "wet" source, as seen by comparing the 355 and 266 nm results for $m=0$ in Fig. 3(b) to those for $n=2$ in Fig. 3(a). This trend persists in the $(CS_2)_n^-$, $n=3-4$, and $(CS_2)_2^-(H_2O)_m$, $m=1-2$, clusters. As seen in Fig. 4, the $(C_2S_2^- + S_2^-)/CS_2^-$ product ratio is always larger within the hydrated cluster series (generated under the wet source conditions) compared to the $(CS_2)_n^-$ series (formed in a dry source).

The large error bars for the $(CS_2)_2^-(H_2O)_m$ parent-ion series in Fig. 4 reflect the variation in the photofragment yields between different experimental runs. These variations result from the day-to-day fluctuations in the concentration of H_2O in the gas delivery lines. No variations in such significant magnitude were observed in the fragmentation patterns when the ion source was kept consistently moisture-free. This observation itself indicates that not just the relative intensities, but also the structural and, therefore, photochemical properties of the $(CS_2)_2^-$ and $(CS_2)_2^-(H_2O)_{1-2}$ cluster anions are affected by the presence of H_2O at the ion formation stage.

The fractional yield of $C_2S_2^-$ from $(CS_2)_2^-$ is positively correlated with the intensity of the C_{2v} $(^2B_1)$ band in the corresponding photoelectron spectrum.[14] Both the $C_2S_2^-$ fragment fraction (at 355 and 266 nm) and the relative intensity of the photoelectron band increase under the wet source conditions. Hence, we conclude that the presence of H_2O in the ion source enhances the formation of the C_{2v} $(^2B_1)$ isomer of $C_2S_4^-$ that in turn gives rise to the $C_2S_2^-$ photofragments.

Summarizing the results, (i) the fractional yield of $C_2S_2^-$ and S_2^- from the bare $(CS_2)_2^-$ parent anion increases in the presence of H_2O at the ion formation stage and (ii) solvation by additional CS_2 or H_2O decreases the fractional yield of the $C_2S_2^-$ and S_2^- fragments, mainly in favor of the CS_2^- channel. Comparing Figs. 3(a) and 3(b), particularly the 355 nm data, it may appear that H_2O is less effective in turning off the $C_2S_2^-$ and S_2^- channels compared to the CS_2 solvent. However, this is largely due to the more abundant presence of the C_{2v} $(^2B_1)$ isomer under the wet source conditions.

IV. DISCUSSION

A. The dissociation channels of $CS_2^-(H_2O)_m$

Similar to the photodissociation of hydrated CO_2^- in water clusters,[16,18] two types of dissociation channels are observed for $CS_2^-(H_2O)_m$ at 355 and 266 nm: (i) the core-dissociation channel, where the CS_2^- cluster core dissociates into S^-+CS accompanied by loss of several water molecules, and (ii) the solvent-evaporation channel, where the photon energy is dissipated by the evaporation of several solvent molecules, while the CS_2^- anion remains intact.

B. The dissociation channels of $(CS_2)_2^-$

In the first photofragmentation experiment on $(CS_2)_2^-$ at photon energies of up to ~2.8 eV, Maeyama *et al.*[6] observed only the CS_2^- and $C_2S_2^-$ fragmentation products. The present findings at 532 nm (2.33 eV) are in line with this result. However, our experiments at 355 and 266 nm reveal additional processes that were not observed previously. First, the $C_2S_2^-$ product channel becomes dominant as the photon energy increases. Second, in addition to CS_2^- and $C_2S_2^-$, we observed new S^-, S_2^-, and CS_3^- products.

These photofragments are plausibly associated with the following pathways:

$$C_2S_4^-(\text{or } CS_2^-\cdot CS_2) + h\nu \rightarrow CS_2^- + CS_2, \quad (1)$$

$$C_2S_4^- + h\nu \rightarrow C_2S_2^- + S_2, \quad (2)$$

$$C_2S_4^- + h\nu \rightarrow S_2^- + C_2S_2, \quad (3)$$

$$CS_2^-\cdot CS_2 + h\nu \rightarrow S^- + CS + CS_2, \quad (4)$$

$$CS_2^-\cdot CS_2 + h\nu \rightarrow CS + S^-\cdot CS_2 \rightarrow CS + CS_3^-. \quad (5)$$

These dissociation channels are summarized in Fig. 5, which shows the proposed reactant structures, intermediates, and products correlations for $(CS_2)_2^-$. Similar pathways, involving additional solvent molecules, are expected for the larger $(CS_2)_n^-$ and $(CS_2)_2^-(H_2O)_m$ clusters.

The parent structures included in Fig. 5 are selected based on the photoelectron imaging results.[14] The relative parent and product-channel energies are from the CCSD(T)/6-311+G(3*df*) calculations.[14,15] The C_{2v} $(^2B_1)$ structure is predicted to be the most stable $(CS_2)_2^-$ structure.[4,14,15] This structure and the next higher-lying one, D_{2h} $(^2B_{3g})$, are characterized by a "doubly excited" electron configuration of the neutral core. That is, the removal of the

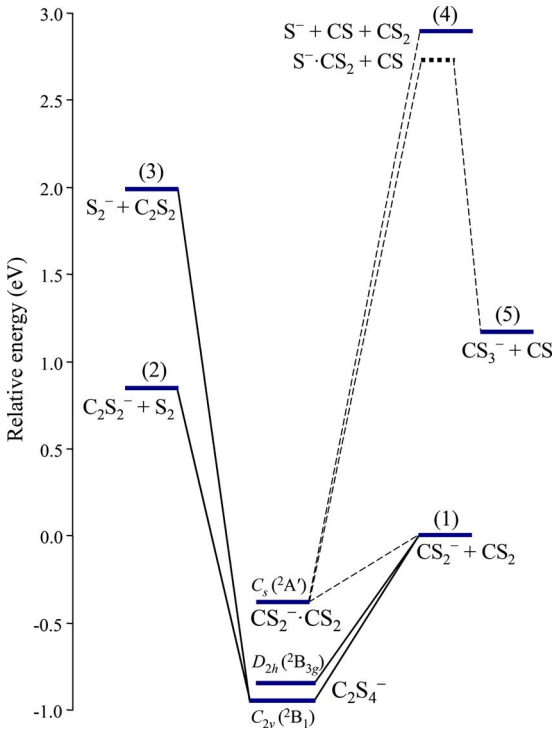

FIG. 5. Energy diagram showing the correlations between the proposed reactant structures, intermediates, and products for the $(CS_2)_2^-$ parent ion. The relative parent and product-channel energies are from the CCSD(T)/6-311+G(3*df*) calculations. The product channel correlations for the $CS_2^-\cdot CS_2$ ion-molecule complex structure (see Fig. 1, top) are shown by dashed lines, while those for the C_{2v} $(^2B_1)$ and D_{2h} $(^2B_{3g})$ isomers (Fig. 1, bottom) are indicated by solid lines. The channel numbers (in parentheses) correspond to the respective pathways indicated by Eqs. (1)–(5) in the text.

excess electron from the highest occupied molecular orbital of either of these anions (in the single-reference picture) yields a doubly excited neutral configuration, rather than that corresponding to two CS_2 molecules in their ground electronic states.[10] The solid lines in Fig. 5 indicate the proposed reactant-product correlations for these doubly excited anionic structures. The correlations of the $CS_2^-\cdot CS_2$ ion-molecule complex, which corresponds to the unexcited ("van der Waals" type) neutral-core configuration,[10] are indicated by the dashed lines.

Figure 5 shows the proposed plausible origins of the final photoproducts without indicating the corresponding excited electronic states. Detailed understanding of the dimer-anion dissociation awaits ingenious theoretical exploration of the excited potential energy surfaces for all the observed electronic structures. For the C_{2v} $(^2B_1)$ global minimum structure, calculations indicate that the dissociation is most likely initiated by the electronic transitions from $X\ ^2B_1$ to the $1\ ^2A_2$, $2\ ^2A_2$, and $^2A_1$ excited states. The $X\ ^2B_1$ state has a double-minimum potential energy curve along the CCS asymmetric bending coordinate. Similar double minima potentials are also predicted for at least some of the excited states.

It follows from Fig. 5 that the appearance of only two anionic fragments, CS_2^- and $C_2S_2^-$, at 532 nm (2.33 eV) can be accounted for by the dissociation energetics. From the mechanistic perspective, channels (1)–(3) are most feasible in the covalent dimer ions, $C_2S_4^-$. It may also be possible to form the CS_2^- photoproduct by predissociation of the $CS_2^-\cdot CS_2$ complex or by caging of the S^-+CS photofragments of its anionic core. Hence, channel (1) can, in principle, involve any of the proposed $(CS_2)_2^-$ isomers. Channels (2) and (3), on the other hand, are most consistent with the lowest-energy C_{2v} $(^2B_1)$ structure, which contains a preexisting S–S bond.

The straightforward mechanism accounting for the S^- fragments is the dissociation of CS_2^- based clusters [channel (4)], analogous to $CO_2^- \rightarrow CO + O^-$ dissociation.[16,18] Channel (5), yielding the CS_3^- photofragments, is also possible in CS_2^- based clusters, assuming that the core dissociation is followed by an ion-molecule association reaction with solvent CS_2. This two-step process is analogous to the CO_3^- channel in $(CO_2)_n^-$ and $(CO_2)_2^-(H_2O)_m$.[3,19]

C. Fragment origins and mechanisms

The S^- and CS_3^- products. In the photodissociation of $CS_2^-(H_2O)_m$, the S^- product is observed for $m=0-5$ at 355 nm [Fig. 2(a)] and for $m=2-5$ at 266 nm [Fig. 2(b)]. For $(CS_2)_2^-$ prepared under the dry source conditions, the S^- product is essentially absent at 355 nm, while CS_3^- is observed [Fig. 3(a)]. The formation of S^- from solvated CS_2^- is possible when, first, the photon energy is large enough to overcome the dissociation threshold and, second, there is sufficient solvent-induced stabilization of excited CS_2^- states (CS_2^{-*}) enabling the $CS_2^{-*} \rightarrow CS + S^-$ dissociation to compete successfully with CS_2^{-*} autodetachment.

By comparing the 266 nm spectra in Fig. 3(a) for $n=2$ and Fig. 3(b) for $m=0$, both of which correspond to (nominally) the same $(CS_2)_2^-$ parent anions, a larger S^- fragment fraction is observed under the dry source conditions. In light of the proposed channel (4) mechanism, this observation parallels the conclusion drawn from the previous photoelectron imaging study,[14] namely, the presence of water in the ion source enhances the formation of the more stable covalent $C_2S_4^-$ dimers over $CS_2^-\cdot CS_2$, of which the latter is primarily responsible for the S^- photofragments. The disappearance of S^- in the $(CS_2)_n^-$, $n=3-4$ fragment mass spectra in Fig. 3(a) reflects, in part, the competition with channel (5), involving a secondary reaction of nascent S^- with the CS_2 solvent.

Based on the mechanism suggested for channel (5), the CS_3^- product intensity should reflect the populations of the CS_2^- based parent clusters, $CS_2^-(CS_2)_{n-1}$, or $CS_2\cdot CS_2^-(H_2O)_m$. Indeed, in Figs. 3(a) and 3(b), the intensity of CS_3^- relative to other photofragments is consistently higher under dry source conditions, compared to the results in a "wet" ion source. Again, this indicates a positive correlation between a process involving a monomeric CS_2^- cluster core and the absence of water in the ion source (even when the parent anions themselves do not contain H_2O).

The largest relative yield of CS_3^- is observed at 266 nm for $(CS_2)_n^-$, $n=3$ and 4, where it is in fact the dominant product. On the other hand, no CS_3^- is observed at the same wavelength from any of the $(CS_2)_2^-(H_2O)_m$ clusters studied, despite the presence of S^- fragments and the availability of a solvent CS_2 molecule for a secondary $S^- + CS_2 \rightarrow CS_3^-$ reaction. This may be a consequence of the structural differences

between the two types of clusters. In $CS_2^-(CS_2)_{n-1}$, more CS_2 molecules become available with increasing n for the secondary S^-+CS_2 association step in Eq. (5), resulting in the observed increase in the CS_3^- fragment intensity from $n=2$ to $n=3-4$. In $CS_2\cdot CS_2^-(H_2O)_m$, on the other hand, the water molecules occupying the most favorable solvation sites near CS_2^- will hinder the secondary reaction.

Although CS_3^- is stable by ~1.7 eV with respect to S^-+CS_2, it was not observed in the drift-tube experiment by Lee and Bierbaum.[5] The authors suggested that due to the large polarizability of CS_2 and relatively low center-of-mass energy, long-lived CS_3^{-*} collision complex could be formed through nucleophilic attack on the carbon. In their experiment, the isotope exchange reaction was observed at collision energies below 0.3 eV, while both the isotope exchange and sulfur abstraction took place above 0.3 eV. The absence of the $^{32}S\ ^{32}S^-$ products above 0.3 eV indicates that the sulfur abstraction occurs through direct attack on the sulfur atom, ruling out the formation of CS_3^{-*}. The observation of CS_3^- in our experiment signals a greater efficiency of the association reaction within a cluster environment, compared to the drift tube experiment.

The CS_2^- product. In the photofragmentation of the $CS_2^-(H_2O)_m$ clusters, CS_2^- fragments are observed for $m\geq 2$ at 355 nm and for $m\geq 3$ at 266 nm (see Fig. 2). The photoinduced excitation of the cluster core should lead to $CS_2^{-*}\rightarrow CS+S^-$ dissociation and/or CS_2^{-*} autodetachment. Since water does not absorb at these wavelengths, the plausible mechanism for CS_2^- fragment formation is via the solvent-induced relaxation of CS_2^{-*} or fragment caging.

The fractional yields of CS_2^- from $(CS_2)_n^-$ and $(CS_2)_2^-(H_2O)_m$ (see Fig. 3) are generally much larger than those from $CS_2^-(H_2O)_m$. This is to be expected, as the dimer based cluster anions are more likely to yield CS_2^- via $C_2S_4^-\rightarrow CS_2^-+CS_2$ dissociation. As seen in Fig. 3, upon addition of CS_2 or H_2O to $(CS_2)_2^-$, the relative yields of the $C_2S_2^-$ and S_2^- channels tend to decrease in favor of CS_2^-. This channel switching is in positive correlation with the decline in the relative intensity of the C_{2v} $(^2B_1)$ photoelectron band.[14,19] This observation indicates the reduced presence of the C_{2v} $(^2B_1)$ core-anion isomer in the larger clusters, compared to the CS_2^- monomer core. There is no clear evidence if the D_{2h} $(^2B_{3g})$ structure is also affected by solvation in a similar manner. On the other hand, the photoelectron imaging results unambiguously show that the fraction of the CS_2^- based parent cluster increases upon solvation.

The $C_2S_2^-$ and S_2^- products. These fragments are expected to be formed from the global-minimum C_{2v} $(^2B_1)$ structure of the $C_2S_4^-$ cluster core. The channel mechanisms may in fact be similar, with the difference being the final localization of the excess electron. The greater (overall) yield of $C_2S_2^-$ and the observed increase in the $(C_2S_2^-+S_2^-)/CS_2^-$ product ratio with increasing photon energy (Fig. 3) are consistent with the S_2^- channel being significantly more endothermic than the $C_2S_2^-$ pathway (Fig. 5).

The $(C_2S_2^-+S_2^-)/CS_2^-$ product ratio plotted in Fig. 4 reflects three important trends. First, in all the cluster anions studied, the ratio increases with increasing photon energy. This trend is consistent with the channel energetics shown in Fig. 5 and therefore favors a statistical mechanism of cluster core photodissociation. Second, for $(CS_2)_2^-$ the above ratio tends to be significantly larger under the wet source conditions, compared to the dry source. The difference is nearly threefold at 266 nm! This observation reinforces our conclusion that the presence of water in the ion source enhances the formation of the most stable C_{2v} $(^2B_1)$ dimer-based clusters, which are responsible for the $C_2S_2^-$ and S_2^- products. Third, solvation of $(CS_2)_2^-$, either by additional CS_2 or by H_2O, leads to a drastic decrease in the $C_2S_2^-$ and S_2^- product yields, relative to the CS_2^- photofragment. The drop in the $C_2S_2^-$ and S_2^- yields is sharper in the CS_2 solvent case: e.g., at all wavelengths studied the $C_2S_2^-$ and S_2^- fragments disappear almost completely with the addition of just one extra CS_2 molecule. This is due to a more abundant formation of the C_{2v} $(^2B_1)$ dimer-based clusters under the wet source conditions compared to that in the dry source.

D. Channel switching versus $(CS_2)_2^-$ isomer coexistence

The variation in the fragment intensities in $(CS_2)_2^-$ dissociation depending on the parent ion source conditions, as well as the observed dominant channel switching from $C_2S_2^-$ and S_2^- to CS_2^- upon salvation, are easily reconciled with the variations in the corresponding photoelectron spectra, reported separately.[14] The dependence of the $(CS_2)_2^-$ fragmentation pattern on the presence of water in the precursor gas line is due to the role of H_2O in facilitating the formation of the global minimum structure of the dimer anion, which dissociates mainly into $C_2S_2^-+S_2$ or $S_2^-+C_2S_2$. In addition to mediating the formation of the equilibrium structure, the water molecules serve as an effective heat sink, stabilizing the residual cluster anion by evaporation. As the photoelectron imaging results indicate,[14] the $(CS_2)_2^-$ anions formed in the dry source are more likely to be trapped in the initially formed, yet less stable $CS_2^-\cdot CS_2$ structure, which is less likely to give rise to the $C_2S_2^-$ and S_2^- products. The formation of the metastable structures, more abundant under the dry source conditions, is attributed to the anion stabilization processes after electron attachment, which mainly involves evaporation of the weakly bound CS_2 molecules or Ar atoms leading to an efficient trapping of the dimer anion in its initially accessible local minima.

When one or more solvent molecules (CS_2 or H_2O) are added to $(CS_2)_2^-$, the relative population of the dimer-core structure declines due to more favorable solvation of CS_2^- versus $C_2S_4^-$. The observed decrease in the $(C_2S_2^-+S_2^-)/CS_2^-$ product ratio reflects the diminishing presence of the global-minimum C_{2v} $(^2B_1)$ core anions upon solvation.

V. SUMMARY

The photodissociation of $(CS_2)_2^-$ at 532, 355, and 266 nm has been investigated using tandem time-of-flight ion mass spectroscopy. Several fragmentation channels are observed, yielding the CS_2^-, $C_2S_2^-$, CS_3^-, S_2^-, and S^- products. The channel branching ratios vary significantly, depending on the presence of water in the precursor gas mixture. Although $(CS_2)_2^-$ itself does not contain H_2O, the observed

variations in the fragmentation patterns reflect the effect of water presence at the ion formation stage on the resulting $(CS_2)_2^-$ isomer distribution. Specifically, the $(C_2S_2^- + S_2^-)/CS_2^-$ channel ratio exhibits a striking positive correlation with the relative intensity of the photoelectron band attributed to the C_{2v} $(^2B_1)$ covalent dimer-anion structure. This $C_2S_4^-$ structure is therefore identified as the primary origin of the $C_2S_2^-$ and S_2^- photoproducts, while the $CS_2^- \cdot CS_2$ ion-molecule complex is seen as the origin of S^- and CS_3^-. The fragmentation patterns also change drastically with the addition of solvent molecules (CS_2 or H_2O) to $(CS_2)_2^-$. Especially striking are the abrupt decrease in the yield of $C_2S_2^-$ and the corresponding increase in the CS_2^- fragment. This solvent-induced channel switching is interpreted in terms of the diminished presence of the covalent $C_2S_4^-$ cluster-core structure relative to the CS_2^- based clusters, due to the more effective solvation of the monomer anion. These results underline the structural complexity of the $(CS_2)_2^-$ anions and complement the parallel photoelectron imaging findings.[14]

ACKNOWLEDGMENTS

We gratefully acknowledge the financial support for this work provided by the National Science Foundation (Grant No. CHE-0713880) and the donors of the ACS Petroleum Research Fund (Grant No. 45406-AC6).

[1] R. G. Keesee and A. W. Castleman, J. Phys. Chem. Ref. Data **15**, 1011 (1986).
[2] J. M. Vandoren, S. E. Barlow, C. H. Depuy, and V. M. Bierbaum, Int. J. Mass Spectrom. Ion Process. **109**, 305 (1991).
[3] L. Velarde, T. Habteyes, and A. Sanov, J. Chem. Phys. **125**, 114303 (2006).
[4] K. Hiraoka, S. Fujimaki, G. Aruga, and S. Yamabe, J. Phys. Chem. **98**, 1802 (1994).
[5] H. S. Lee and V. M. Bierbaum, J. Chem. Phys. **101**, 9513 (1994).
[6] T. Maeyama, T. Oikawa, T. Tsumura, and N. Mikami, J. Chem. Phys. **108**, 1368 (1998).
[7] T. Tsukuda, T. Hirose, and T. Nagata, Chem. Phys. Lett. **279**, 179 (1997).
[8] S. Koizumi, H. Yasumatsu, S. Otani, and T. Kondow, J. Phys. Chem. A **106**, 267 (2002).
[9] Y. Kobayashi, Y. Inokuchi, and T. Ebata, J. Chem. Phys. **128**, 164319 (2008).
[10] A. Sanov, W. C. Lineberger, and K. D. Jordan, J. Phys. Chem. A **102**, 2509 (1998).
[11] R. Mabbs, E. Surber, and A. Sanov, Chem. Phys. Lett. **381**, 479 (2003).
[12] L. A. Yu, A. H. Zeng, Q. A. Xu, and M. F. Zhou, J. Phys. Chem. A **108**, 8264 (2004).
[13] S. W. Zhang, C. G. Zhang, Y. T. Yu, B. Z. Mao, and F. C. He, Chem. Phys. Lett. **304**, 265 (1999).
[14] T. Habteyes, L. Velarde, and A. Sanov, J. Phys. Chem. A **112**, 10134 (2008).
[15] T. Habteyes, Ph.D. dissertation, University of Arizona, 2008.
[16] T. Habteyes, L. Velarde, and A. Sanov, Chem. Phys. Lett. **424**, 268 (2006).
[17] M. A. Johnson and W. C. Lineberger, in *Techniques for the Study of Ion Molecule Reactions*, edited by J. M. Farrar and W. H. Saunders (Wiley, New York, 1988), p. 591.
[18] T. Habteyes, L. Velarde, and A. Sanov, J. Chem. Phys. **126**, 154301 (2007).
[19] M. L. Alexander, M. A. Johnson, N. E. Levinger, and W. C. Lineberger, Phys. Rev. Lett. **57**, 976 (1986).